How to cite: *Angew. Chem. Int. Ed.* **2025**, *64*, e202424166
doi.org/10.1002/anie.202424166

VIP Diradicals Very Important Paper

Ph_3PC – A Monosubstituted C(0) Atom in Its Triplet State

Yury Kutin, Taichi Koike, Maria Drosou, Alexander Schnegg, Dimitrios A. Pantazis, Müge Kasanmascheff,* and Max M. Hansmann**

Dedicated to Prof. Dr. Wolfram Sander on the occasion of his 70th birthday.

Abstract: This study introduces a novel class of carbon-centered diradicals: a monosubstituted C atom stabilized by a phosphine. The diradical $Ph_3P{\rightarrow}C$ was photochemically generated from a diazophosphorus ylide precursor (Ph_3PCN_2) and characterized by EPR and isotope-sensitive ENDOR spectroscopy at low temperatures. $Ph_3P{\rightarrow}C$ features an axial zero-field splitting parameter $D = 0.543\ cm^{-1}$ with a vanishingly small rhombicity $|E|/D = 0.002$. Time- and temperature-dependent measurements confirm a triplet ground state with a lifetime of approximately 10 min at 127 K in toluene-d_8. Multireference electronic structure calculations predict a clear triplet ground state with a singlet-triplet gap greater than 20 kcal/mol. In contrast to divalent C(0) compounds, such as $Ph_3P{\rightarrow}C{\leftarrow}PPh_3$, in which carbon needs excitation into a highly-excited closed-shell $2s^0 2p^4$ configuration, $Ph_3P{\rightarrow}C$ can be explained by direct involvement of carbon in its natural ^3P state arising from the $2s^2 2p^2$ configuration.

Tuning the oxidation number and valency of carbon is a key factor for creating fundamental new compounds and opening up novel reactivities and photophysical properties. Very recent contributions show the flourishing chemistry of fundamental carbon-based compounds, for instance a phosphine-stabilized C_2 species,[1] a divalent doubly oxidized carbene,[2] or a metallocarbene with an inverted electronic state.[3] Divalent C(II) compounds (carbenes), which only contain six valence electrons around the C(II) center, can exist in both the singlet and triplet ground state (Scheme 1a). Several room-temperature stable singlet carbenes have been reported,[4] with a long list of applications in different areas of chemistry and beyond. Besides a few exceptions,[5] triplet carbenes are typically studied as reactive intermediates at low temperatures, often in frozen organic solvents or using matrix-isolation techniques.[6]

A topologically related case is the closed-shell divalent C(0) compound in which carbon contains two lone-pairs flanked by two neutral donor ligands. A seminal example is the class of carbodiphosphoranes (Scheme 1b).[7] Frenking and co-workers interpreted their electronic structure as C(0) compounds (carbones) in which two two-electron donor ligands add into a carbon atom in its excited, closed-shell $2s^0 2p^4$ configuration.[8]

Considering the dative ligand representation and the recently developed concept of exchange reactions at carbon,[10] we were curious whether formal dissociation of a PPh_3 moiety from $Ph_3P{\rightarrow}C{\leftarrow}PPh_3$ could lead to $Ph_3P{\rightarrow}C$, representing an open-shell monovalent C(0) atom. While

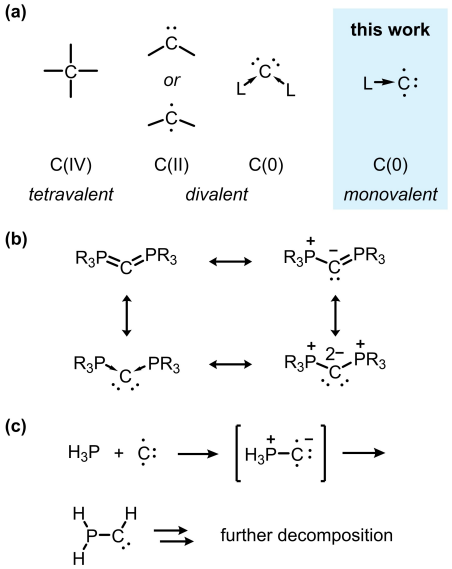

Scheme 1. (a) Common valencies and oxidation states of carbon, (b) resonance structures of carbodiphosphoranes, and (c) molecular cross beam experiment of atomic carbon with H_3P.[9]

[*] Dr. Y. Kutin, Dr. T. Koike, Prof. Dr. M. Kasanmascheff, Prof. Dr. M. M. Hansmann
Department of Chemistry and Chemical Biology
Technische Universität Dortmund
Otto-Hahn-Str.6, 44227 Dortmund, Germany
E-mail: muege.kasanmascheff@tu-dortmund.de
max.hansmann@tu-dortmund.de

Dr. M. Drosou, Dr. D. A. Pantazis
Max-Planck-Institut für Kohlenforschung
Kaiser-Wilhelm-Platz 1, 45470 Mülheim an der Ruhr, Germany
E-mail: dimitrios.pantazis@kofo.mpg.de

Dr. A. Schnegg
Max-Planck-Institute for Chemical Energy Conversion
Stiftstrasse 34–36, 45470 Mülheim an der Ruhr, Germany

monovalent compounds of main-group elements, such as the recent work on triplet nitrenes (R–N),[11] triplet arsinidenes (R–As),[12] or triplet bismuthinidenes (R–Bi),[13] are a very active research area, a monovalent diradical carbon(0) atom represents an unknown molecule class, with the exception of a triplet vinylidene.[14] The parent molecule H_3PC has been proposed to form in interstellar space and was computationally investigated.[15] Kaiser and co-workers performed a crossed molecular beam reaction of ground-state carbon atoms $C(^3P_j)$ with PH_3 (X^1A_1), which proceeds on the triplet surface via barrierless H_3P–C formation but undergoes further hydrogen shift reactions (Scheme 1c).[9] In this study, we report the first low-temperature characterization of $Ph_3P{\rightarrow}C$ by electron paramagnetic resonance (EPR) and isotope-sensitive electron-nuclear double resonance (ENDOR) spectroscopy, supported by quantum chemical calculations.

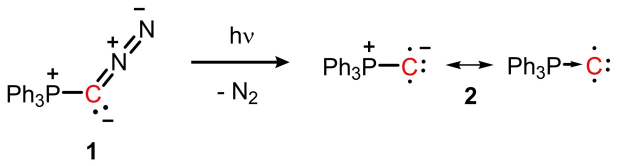

Scheme 2. Synthesis of monosubstituted $Ph_3P{\rightarrow}C$ by light-triggered dinitrogen elimination.

Accessing the $Ph_3P{\rightarrow}C$ diradical through ligand dissociation from $Ph_3P{\rightarrow}C{\leftarrow}PPh_3$ appears unlikely, while reactions with atomic carbon are challenging to perform and bear the risk of being unselective due to the high reactivity of atomic carbon.[16] Therefore, we targeted a clean and straightforward synthetic route by photochemically liberating dinitrogen from our recently reported diazophosphorus ylide **1** (Scheme 2).[17]

The diazophosphorus ylide precursor **1** was illuminated with UV light at cryogenic temperatures in a frozen MeTHF solution. The resulting photolysis products were analyzed using continuous wave (CW) and electron-spin echo (ESE)-detected EPR spectroscopy at the X-band (9.4 GHz), Q-band (34 GHz) and W-band (94 GHz) frequencies. The collected EPR spectra, shown in Figure 1 along with simulations, demonstrate the formation of a triplet species. This triplet species remained unchanged at 6 K for several days after the initial UV illumination. Temperature-dependent measurements were performed in the range of 10 to 60 K at X-band. A Curie–Weiss plot (Figure 1a, inset) exhibits a linear dependence, consistent with a triplet ground state.

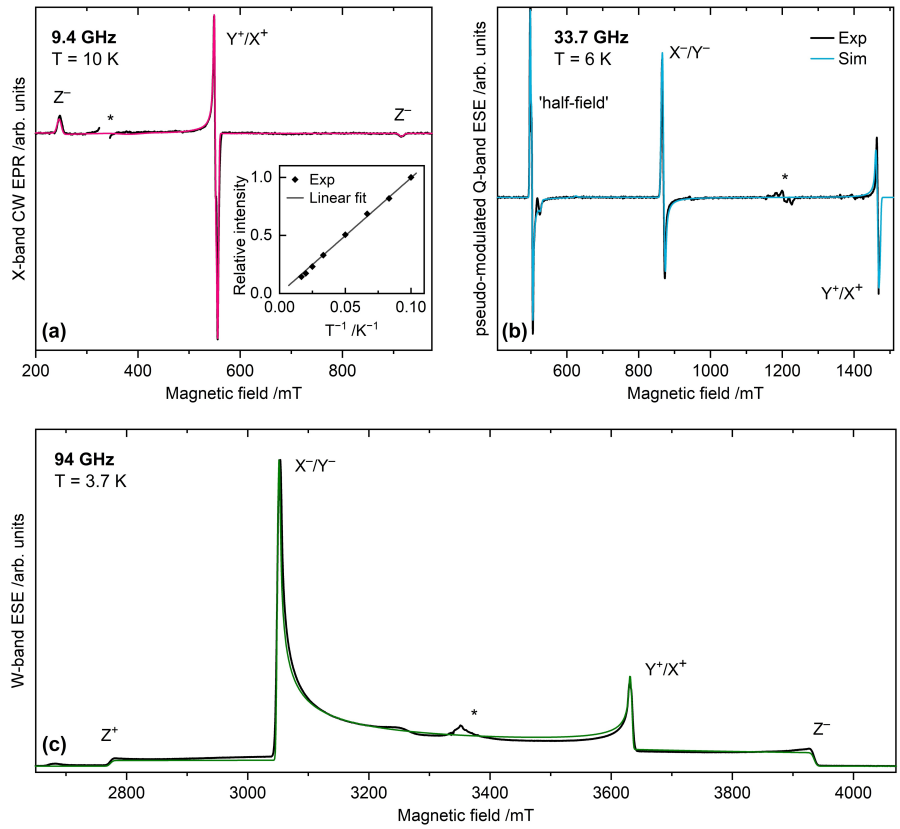

Figure 1. (a) CW X-band, (b) ESE-detected Q-band, and (c) ESE-detected W-band EPR spectra (black solid lines) of **2** in a frozen MeTHF solution. The spectra are overlaid with the best fits obtained assuming an $S=1$ species and $g_{iso}=2.0023$ (lines of various colors). The Q-band trace was pseudo-modulated to highlight the narrow spectral features; the simulated "half-field" signal intensity was reduced to account for a difference in transition probabilities. Inset: CW EPR intensity of the Y^+/X^+ feature *vs.* inverse temperature between 10 and 60 K with a linear fit. The asterisks mark a radical signal at $g\approx2$.

The zero-field splitting (ZFS) parameters D and E/D, obtained from a global fit of the EPR data collected at the three frequencies, are given in Table 1. Multi-frequency EPR was crucial for precisely determining these parameters (see Figure S2.1 for the frequency dependence of the spectrum). At Q-band, the position of the Y^+/X^+ EPR line coincided with the limit of a standard resistive EPR magnet (Figure 1b). To overcome this limitation and detect the entire Pake pattern, as well as determine the sign of D from thermal polarization, W-band EPR (field range of 0–6 T) was employed (Figure 1c). Additionally, the X-band EPR data enabled accurate constraint of the small E value (see Figure S2.2). The experimentally fitted ZFS values agree well with the ones computed with multireference 2nd-order N-electron valence state perturbation theory (NEVPT2) in the framework of quasi-degenerate perturbation theory (see below).

To contextualize the determined ZFS parameter $D = 0.543\ cm^{-1}$ for **2**, we compared it with other diradical classes. The detected value is lower than that of triplet methylene (CH_2; $D = 0.69\ cm^{-1}$; $|E|/D = 0.004$; in Xe matrix at 4 K)[18] but close to the value reported for phenylcarbene ($D = 0.515\ cm^{-1}$, $|E|/D = 0.049$).[19] Diphenylcarbenes, on the other hand, typically exhibit lower D values in the range of 0.35–0.41 cm^{-1}.[6b] Notably, the determined D value for **2** is approximately 40 % higher than that of our recently described triplet vinylidene ($D = 0.377\ cm^{-1}$).[14] This comparison highlights the distinct electronic structure and properties of **2** within the broader context of related species.

To probe the electronic structure of **2**, the hyperfine (hf) coupling tensors were determined using the Davies ENDOR technique at Q-band (see Figures 2 and S2.3). The ^{31}P isotope, with nuclear spin $I = 1/2$ and 100 % natural abundance, provided the perfect opportunity for an ENDOR investigation. The narrow, well-defined ENDOR lines with a clear field dependence were assigned to the ^{31}P nucleus. The ^{31}P hf tensor given in Table 1 (with the computational values listed below) provided an excellent fit at every field position. It is dominated by an isotropic component $A_{iso}(^{31}P) = -105.3$ MHz. Note that while the Z^+ spectral feature is not well-defined at Q-band due to a large D value, and the Z^- feature is beyond the magnet's limit, the A_Z tensor components could be determined from several ENDOR measurements within the "half-field" transition. The Davies ENDOR data obtained for a natural-abundance sample, containing only ^{31}P and ^{1}H transitions are shown in Figure S2.3. The broad, unresolved ^{1}H ENDOR features originate from the phenyl-ring protons and are not discussed further.

Table 1: ZFS and hf parameters of **2** providing the best global fit to the multifrequency EPR and Q-band ENDOR data;[a] calculated ZFS (with NEVPT2 in the framework of quasi-degenerate perturbation theory) and hf (with DLPNO-CCSD) parameters of **2**. [a]The uncertainties in the simulated values are ±0.5 MHz for the hf tensor components, ±0.003 cm^{-1} for D, and ±0.001 for $|E|/D$. The simulations of experimental data were performed assuming $g_{iso} = 2.0023$; the ZFS and the two hf tensors were assumed collinear.

	ZFS		^{31}P hf (MHz)			^{13}C hf (MHz)		
	D (cm^{-1})	$\|E\|/D$	A_X	A_Y	A_Z	A_X	A_Y	A_Z
Exp.	+0.543	0.002	−102.4	−102.4	−111.2	76.7	76.7	−17.9
Calc.	+0.549	0.000	−113.3	−113.3	−122.7	60.0	59.9	−33.1

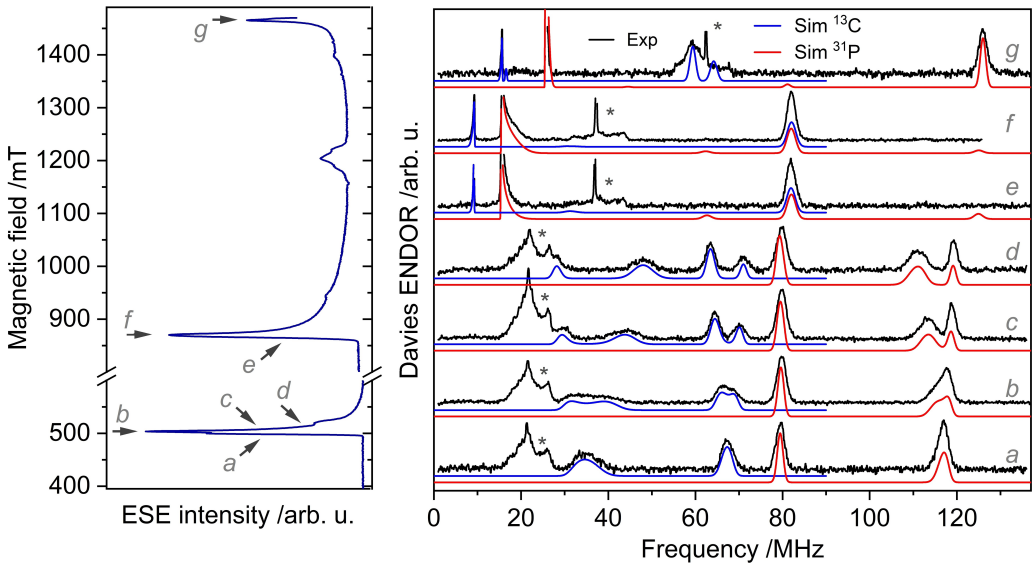

Figure 2. Davies ENDOR spectra of **2** acquired at three canonical field positions (*e–g*: 865, 873, 1467 mT) and four positions within the "half-field" feature (*a–d*: 500, 505, 508, 513 mT, black traces) overlaid with simulated ^{31}P and ^{13}C spectra (red and blue traces, respectively). Asterisks mark ^{1}H features. ^{31}P and ^{13}C hf parameters are given in Table 1.

Having identified the phosphorus-related ENDOR lines, we repeated the measurements on a selectively ^{13}C-labeled sample ($Ph_3P^{13}CN_2$), which further constrained the electronic structure (Figures 2 and S2.4–2.6). In addition to the known ^{31}P features, new spectral lines were found in each trace, which were assigned to the terminal ^{13}C nucleus. These ^{13}C spectral features were simulated using the hf tensor given in Table 1. The isotropic hyperfine component $A_{iso}(^{13}C)$ of **2** is approximately 45 MHz, similar to that observed for triplet vinylidenes (≈50 MHz),[14] but relatively low compared to that of triplet carbenes. E.g., the $A_{iso}(^{13}C)$ values reported for triplet methylene (CH_2), diphenylcarbene, and fluorenylidene are 250,[20] 173,[21] and 263 MHz, respectively.[22]

Quantum chemical calculations were performed on **2** with Orca[23] using the orbital-optimized and spin-component scaled OO-RI-SCS-MP2/def2-TZVP approach,[24–26] which has been previously benchmarked for a reference set of aryl carbenes.[27–28] Spin state energetics and ZFS parameters were obtained from multireference NEVPT2[29–30] calculations on the basis of complete active space self-consistent field (CASSCF) wavefunctions with an active space of 4 electrons in 6 orbitals. These calculations suggest that the triplet ground state is separated by more than 20 kcal mol^{-1} from excited singlet states.

Focusing on the P–C bond, the optimizations result in bond length of 1.77 Å and the computed Mayer bond order from our multireference calculations is 1.4, indicative of multiple-bond character. Analysis of the bonding (Figure 3) suggests that it can be understood in terms of a triplet C atom in its ground state (^{3}P state arising from the $2s^22p^2$ configuration) accepting the lone pair from Ph_3P (in its ground ^{1}A state) leading to a ^{3}A state of the adduct **2**. The two unpaired electrons reside originally at the p_x, p_y orbitals of C, both perpendicular to the σ-orbital created by the donation of the P lone pair to the empty p_z orbital of C. There is partial delocalization of spin density on P due to back-donation from the C $2p_x$ and $2p_y$ orbitals to the empty P–Ph antibonding orbitals (Figure 3b), reflected in the shapes of the final π_x and π_y orbitals of the adduct (Figure 3a) and in the total spin density distribution and spin populations computed for C and P (ca. 1.7 and 0.2 electrons, respectively, Figure 3c). Natural bond orbital (NBO) analysis[31] (see Supporting Information 3.2) confirms the description of the bonding, quantifying the atomic orbital contributions and the magnitude of backdonation.

There has been a vivid discussion of dative or electron-sharing bonding in main-group compounds.[32] To analyze this computationally for the P–C bond in **2** (Lewis structures in Scheme 2), we employ the IUPAC definition and study the different dissociation possibilities. The calculated (B3LYP/def2-TZVP) dissociation energy of **2** to the neutral fragments Ph_3P in its ground singlet state and atomic C in its ground triplet (^{3}P) state is 56 kcal mol^{-1}, whereas homolytic dissociation to the cationic radical Ph_3P^+ and the spin-quartet anionic C^- is 197 kcal mol^{-1}. Therefore, dissociation of the P–C bond in **2** would be heterolytic, and hence the P–C bond is best described as a dative bond. Energy decomposition analysis (EDA) also shows that the interaction energy of the closed-shell Ph_3P and ground-state C fragments is considerably more favorable compared to the open shell doublet Ph_3P^+ and quartet C^- (see Supporting

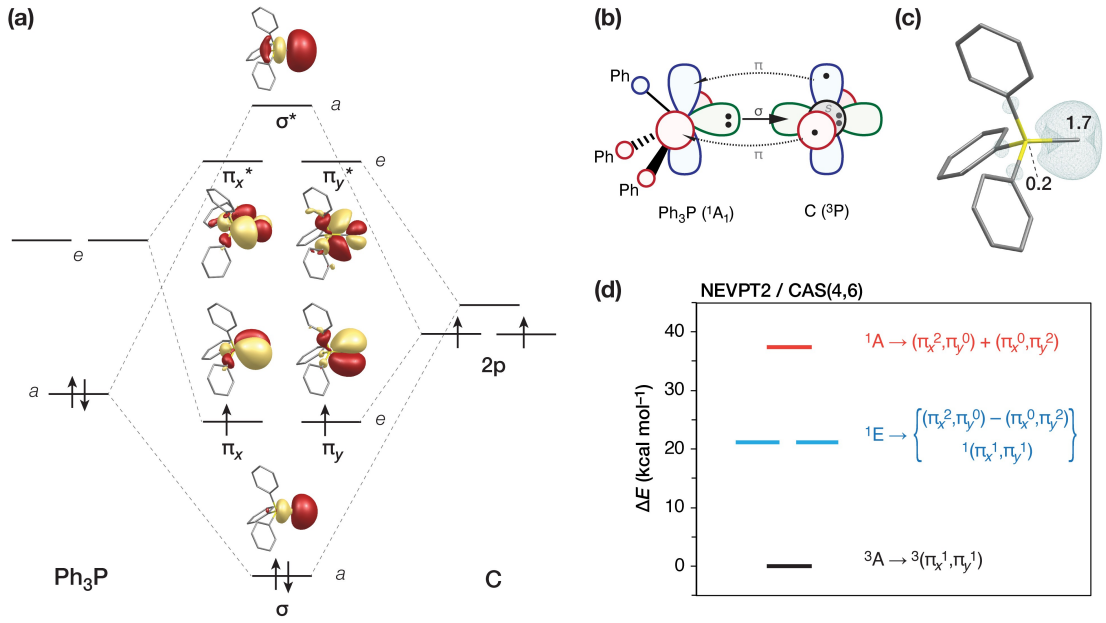

Figure 3. (a) Orbital interaction diagram between Ph_3P (^{1}A) and ground-state atomic C (^{3}P) forming triplet Ph_3P–C (orbitals from CASSCF(4,6) calculations). (b) Bonding interactions indicating σ-donation from P to C and π-back-donation from the singly occupied orthogonal C p-orbitals to antibonding orbitals of Ph_3P. (c) Spin density of the triplet Ph_3P–C, calculated with DLPNO-CCSD, showing symmetric distribution of spin around the C atom and small spin delocalization on P. (d) Location and nature of excited spin-singlet states from multireference NEVPT2/CASSCF(4,6) calculations. Excited singlet states are represented by linear combinations of open- and closed-shell configurations involving the π_x and π_y orbitals.

Information 3.3). We note that a heterolytic bond dissociation pathway has also been described for the H_3P–C molecule.[15a] The direct involvement of a ground-state C atom in $Ph_3P{\rightarrow}C$ explains straightforwardly why the monovalent carbon adduct maintains a triplet ground state. This situation is to be contrasted with the case of the divalent carbon in "carbones",[8] where the bonding is instead discussed as arising from two dative bonds to a C atom in a hypothetical highly-excited closed-shell $2\,s^0 2p^4$ configuration.

Table 1 reports hyperfine coupling tensors obtained with the highest applicable level of theory available to us, the domain-based local pair natural orbital approximation to coupled-cluster theory with singles and doubles excitations, DLPNO-CCSD.[33,34] The results agree well with the experimentally determined hyperfine coupling constants for ^{31}P and ^{13}C, reproducing closely both the magnitude and the symmetry. The reason for the significantly smaller $A_{iso}(^{13}C)$ in **2** compared to those of triplet carbenes (Table S3.2) is the greatly reduced spin density on the C nucleus, since both unpaired electrons reside on orbitals of p character. The unpaired electrons on C induce spin polarization along the σ bond between P and C, resulting in the localization of α spin on the p_z orbital of C and β spin on the P nucleus, which explains the negative $A_{iso}(^{31}P)$.

The present P–C system is characterized by a purely axial ^{13}C hf tensor, consistent with the fact that the two perpendicular components that involve the singly occupied C p_x and p_y orbitals (Figure 3) are perfectly equivalent. This cylindrical symmetry of the p components contrasts with the previously described vinylidene,[14] where one of the p orbitals of C is incorporated in an extended π-system (see Figure S3.2) resulting in significant spin delocalization in one direction, whereas the other is a non-bonding in-plane orbital fully localized on C. This unequal distribution of unpaired electrons in vinylidenes leads to a high rhombicity in this family of compounds. Therefore, the varying degree of differentiation between the two singly occupied carbon p orbitals that are perpendicular to the σ-bonding component is a key contributor to the rhombicity of the hyperfine tensor by affecting the anisotropy in the spin distribution.

EPR measurements presented thus far were conducted at temperatures ≤ 60 K, where the triplet species **2** is stable. An overnight annealing experiment, in which the sample was held at an elevated temperature, revealed no observable decay of **2** up to at least 70 K (Figure S2.7). To further assess the stability of **2** in MeTHF, the intensity of the Y^+/X^+ feature was monitored at various temperatures via EPR measurements using a nitrogen-cooled X-band EPR spectrometer. In MeTHF, the EPR intensity decayed almost completely after 1 h at 94 K, the lowest achievable temperature limited by the experimental setup (Figure 4). The monoexponential decay of the EPR intensity could be simulated with a rate constant of $k = 0.044(1)\ min^{-1}$ (fitting parameters presented in Table S2.1). In contrast, a higher stability of **2** was observed in toluene at 94 K, with a rate constant of $k = 0.003(1)\ min^{-1}$. This enhanced stability in toluene can be attributed to its relatively high glass transition temperature (117 K) compared to MeTHF

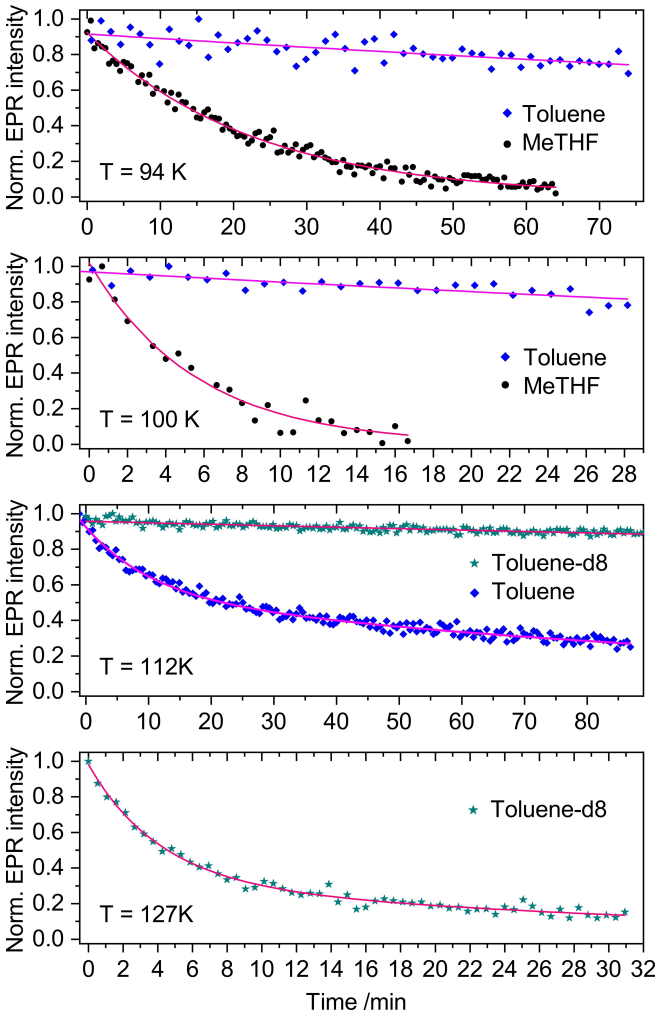

Figure 4. Isothermal decay of the triplet species **2** at 94, 100, 112 and 127 K in the various solvents monitored via intensity of the Y^+/X^+ spectral feature at X-band. A mono- or biexponential function was used to fit the experimental data (see Table S2.1).

(91 K).[35] Furthermore, the triplet species **2** exhibited increased stability in deuterated toluene, indicating that its decay proceeds via a reaction with the solvent molecules, such as H-atom abstraction or C–H insertion.

Performing the irradiation (390 nm) in a J-Young NMR tube led to a complex reaction mixture with the generation of triphenylphosphine as the main decomposition product (23 % yield based on NMR integrals, Figure S1.1–1.2), which hints toward a P–C bond cleavage in the course of the reaction. The formation of an initial dimer of **2** was suggested from HRMS measurements of the crude mixture after irradiation [ESI(+) $[M+H]^+$ $C_{38}H_{31}P_2^+$ calc. 549.1896, found 549.1919; APCI(+) $[M+H]^+$ found 549.1902, Figure S1.3]. However, monitoring the irradiation reaction of **^{13}C-2** in THF-d_8 at −50 °C in the NMR spectrometer already gave rise to numerous decomposition products and the characterization of initial decomposition intermediates proved challenging. Initial trapping experiments with small organic molecules were challenging due to the high

reactivity of both **1** and **2** and typically resulted in a complex mixture with the major product being PPh_3 (see Chart S1.1).

In summary, irradiation of the phosphorus diazo precursor **1** followed by EPR and ENDOR detection gives clear evidence for a new carbon diradical class, a monovalent C atom flanked by a PPh_3 moiety ($Ph_3P{\rightarrow}C$). While for the bonding in carbones ($L{\rightarrow}C{\leftarrow}L$) carbon is required to be in a high-lying energetic $2s^02p^4$ configuration, the bonding in ($L{\rightarrow}C$) can be explained with carbon being in its natural ^3P ground state ($2s^22p^2$). Considering the advantage of diradicals/high-spin systems to be interesting materials for spin/magnetic devices,[36] future work will address tuning the stability as well as applications. Additionally, it remains to be investigated if such a new diradical compound class could also be used as reactive intermediates in synthetic organic chemistry.

Acknowledgements

The Max Planck Society (D.A.P. and A.S.) and the Alexander von Humboldt Foundation (fellowships to T.K. and M.D.) are thanked for financial support. We thank Thilo Hetzke and Sylwia Kacprzak from Bruker BioSpin for providing access to their X-band EPR spectrometer. Leonid Rapatskiy is acknowledged for his assistance with the W-band illumination set-up. Bastian Grabe is thanked for help with irradiation inside the NMR spectrometer. Christian Sindlinger is acknowledged for help with the ADF calculation. This work is funded by the Deutsche Forschungsgemeinschaft (DFG, German Research Foundation) under Germany's Excellence Strategy – EXC 2033–390677874 – RESOLV (to M.K. and M.M.H) and the European Research Council (ERC-StG "CC–CHARGED" 101077332; to M.M.H.). Open Access funding enabled and organized by Projekt DEAL.

Conflict of Interest

The authors declare no conflict of interest.

Data Availability Statement

The data that support the findings of this study are available in the supplementary material of this article.

Keywords: reactive intermediates · carbon · EPR spectroscopy · diradicals · carbones

[1] T.-F. Leung, D. Jiang, M.-C. Wu, D. Xiao, W.-M. Ching, G. P. A. Yap, T. Yang, L. Zhao, T.-G. Ong, G. Frenking, *Nat. Chem.* **2021**, *13*, 89–93.
[2] Y. K. Loh, M. Melaimi, M. Gembicky, D. Munz, G. Bertrand, *Nature* **2023**, *623*, 66–70.
[3] C. Hu, X.-F. Wang, J. Li, X.-Y. Chang, L. L. Liu, *Science* **2024**, *383*, 81–85.
[4] a) A. Igau, H. Grutzmacher, A. Baceiredo, G. Bertrand, *J. Am. Chem. Soc.* **1988**, *110*, 6463–6466; b) A. J. Arduengo III, R. L. Harlow, M. A. Kline *J. Am. Chem. Soc.* **1991**, *113*, 361–363; c) D. Bourissou, O. Guerret, F. P. Gabbai, G. Bertrand, *Chem. Rev.* **2000**, *100*, 39–92.
[5] H. Tomioka, E. Iwamoto, H. Itakura, K. Hirai, *Nature* **2001**, *412*, 626–628.
[6] a) K. Hirai, T. Itoh, H. Tomioka, *Chem. Rev.* **2009**, *109*, 3275–3332; b) W. Sander, G. Bucher, S. Wierlacher, *Chem. Rev.* **1993**, *93*, 1583–1621.
[7] a) F. Ramirez, N. B. Desai, B. Hansen, N. McKelvie, *J. Am. Chem. Soc.* **1961**, *83*, 3539–3540; b) H. Schmidbaur, O. Gasser, M. S. Hussain, *Chem. Ber.* **1977**, *110*, 3501–3507; c) R. Appel, U. Baumeister, F. Knoch, *Chem. Ber.* **1983**, *116*, 2275–2284; d) O. Gasser, H. Schmidbaur, *J. Am. Chem. Soc.* **1975**, *97*, 6281–6282.
[8] a) R. Tonner, F. Öxler, B. Neumüller, W. Petz, G. Frenking, *Angew. Chem. Int. Ed.* **2006**, *45*, 8038–8042; b) S. Klein, R. Tonner, G. Frenking, *Chem. Eur. J.* **2010**, *16*, 10160–10170; c) W. Petz, G. Frenking, *Carbodiphosphoranes and Related Ligands. In: R. Chauvin, Y. Canac, (eds) Transition Metal Complexes of Neutral eta1-Carbon Ligands. Topics in Organomet. Chem.* **2010**, *30*, Springer, Berlin, Heidelberg; d) G. Frenking, R. Tonner, *Pure Appl. Chem.* **2009**, *81*, 597–614.
[9] Y. Guo, X. Gu, F. Zhang, B. J. Sun, M. F. Tsai, A. H. H. Chang, R. I. Kaiser, *J. Phys. Chem. A* **2007**, *111*, 3241–3247.
[10] a) P. W. Antoni, C. Golz, J. J. Holstein, D. A. Pantazis, M. M. Hansmann, *Nat. Chem.* **2021**, *13*, 587–593; b) P. W. Antoni, J. Reitz, M. M. Hansmann, *J. Am. Chem. Soc.* **2021**, *143*, 12878–12885; c) W. Feuerstein, P. Varava, F. Fadaei-Tirani, R. Scopelliti, K. Severin, *Chem. Commun.* **2021**, *57*, 11509–11512; d) R. Wei, X. Wang, D. A. Ruiz, L. L. Liu, *Angew. Chem. Int. Ed.* **2023**, *62*, e202219211; e) for a review on ligand exchange at carbon, see: F. Krischer, V. H. Gessner, *JACS Au* **2024**, *4*, 1709–1722.
[11] a) M. Janssen, T. Frederichs, M. Olaru, E. Lork, E. Hupf, J. Beckmann, *Science* **2024**, *385*, 318–321; b) D. Wang, W. Chen, H. Chen, Y. Chen, S. Ye, G. Tan, *Nat. Chem.* **2025**, *17*, 38–43.
[12] a) W. Qian, P. R. Schreiner, A. Mardyukov, *J. Am. Chem. Soc.* **2023**, *145*, 12755–12759; b) W. Qian, P. R. Schreiner, A. Mardyukov, *J. Am. Chem. Soc.* **2024**, *146*, 930–935.
[13] a) Y. Pang, N. Nöthling, M. Leutzsch, L. Kang, E. Bill, M. van Gastel, E. Reijerse, R. Goddard, L. Wagner, D. SantaLucia, S. DeBeer, F. Neese, J. Cornella, *Science* **2023**, *380*, 1043–1048; b) M. Wu, W. Chen, D. Wang, Y. Chen, S. Ye, G. Tan, *Natl. Sci. Rev.* **2023**, *10*, nwad169.
[14] Y. Kutin, J. Reitz, P. W. Antoni, A. Savitsky, D. A. Pantazis, M. Kasanmascheff, M. M. Hansmann, *J. Am. Chem. Soc.* **2021**, *143*, 21410–21415.
[15] a) R. Rey-Villaverde, S. Álvarez-Barcia, J. R. Flores, *J. Chem. Phys.* **2012**, *137*, 014316; b) R. Rey-Villaverde, H. Cybulski, J. R. Flores, B. Fernández, *Comp. Chem.* **2013**, *34*, 2020–2031.
[16] a) C. Mackay, R. Wolfgang, *Science* **1965**, *148*, 899–907; b) K. J. Klabunde, *"Carbon, silicon, germanium, tin, and lead (group IVA)" in Free Chemistry of Free Atoms and Particles*, K. J. Klabunde, Ed. **1980**, 179–210; c) P. S. Skell, J. J. Havel, M. J. McGlinchey, *Acc. Chem. Res.* **1973**, *6*, 97–105.
[17] T. Koike, J.-K. Yu, M. M. Hansmann, *Science* **2024**, *385*, 305–311.
[18] R. A. Bemheim, H. W. Bernard, P. S. Wang, L. S. Wood, P. S. Skell, *J. Chem. Phys.* **1970**, *53*, 1280–1281.
[19] E. Wasserman, A. M. Trozzolo, W. A. Yager, *J. Chem. Phys.* **1964**, *40*, 2408–2410.
[20] R. A. Bernheim, H. W. Bernard, P. S. Wang, L. S. Wood, P. S. Skell, *J. Chem. Phys.* **1971**, *54*, 3223–3225.
[21] R. W. Brandon, G. L. Closs, C. E. Davoust, C. A. Hutchison, B. E. Kohler, R. Silbey, *J. Chem. Phys.* **1965**, *43*, 2006–2016.

[22] E. Wasserman, A. M. Trozzolo, W. A. Yager, R. W. Murray, *J. Chem. Phys.* **1964**, *40*, 2408–2410.
[23] F. Neese, F. Wennmohs, U. Becker, C. Riplinger, *J. Chem. Phys.* **2020**, *152*, 224108.
[24] W. Kurlancheek, M. Head-Gordon, *Mol. Phys.* **2009**, *107*, 1223–1232.
[25] F. Neese, T. Schwabe, S. Kossmann, B. Schirmer, S. Grimme, *J. Chem. Theory Comput.* **2009**, *5*, 3060–3073.
[26] S. Grimme, *J. Chem. Phys.* **2003**, *118*, 9095–9102.
[27] R. Ghafarian Shirazi, D. A. Pantazis, F. Neese, *Mol. Phys.* **2020**, *118*, e1764644.
[28] R. Ghafarian Shirazi, F. Neese, D. A. Pantazis, *J. Chem. Theory Comput.* **2018**, *14*, 4733–4746.
[29] C. Angeli, R. Cimiraglia, S. Evangelisti, T. Leininger, J.-P. Malrieu, *J. Chem. Phys.* **2001**, *114*, 10252–10264.
[30] C. Angeli, R. Cimiraglia, J.-P. Malrieu, *Chem. Phys. Lett.* **2001**, *350*, 297–305.
[31] F. Weinhold, C. R. Landis, *Valency and Bonding: A Natural Bond Orbital Donor-Acceptor Perspective*, Cambridge University Press, Cambridge, 2005, p. 749.
[32] a) G. Frenking, *Angew. Chem. Int. Ed.* **2014**, *53*, 6040–6046; b) D. Himmel, I. Krossing, A. Schnepf, *Angew. Chem. Int. Ed.* **2014**, *53*, 370–374.
[33] C. Riplinger, F. Neese, *J. Chem. Phys.* **2013**, *138*, 034106.
[34] M. Saitow, F. Neese, *J. Chem. Phys.* **2018**, *149*, 034104.
[35] L. M. Wang, C. A. Angell, R. Richert, *J. Chem. Phys.* **2006**, *125*, 074505.
[36] M. Abe, *Chem. Rev.* **2013**, *113*, 7011–7088.

Manuscript received: December 10, 2024
Accepted manuscript online: January 27, 2025
Version of record online: February 9, 2025